JOURNAL OF VIROLOGY, May 2004, p. 5088–5096 Vol. 78, No. 10
0022-538X/04/$08.00+0 DOI: 10.1128/JVI.78.10.5088–5096.2004

Differential Cell Killing by Lymphomagenic Murine Leukemia Viruses Occurs Independently of p53 Activation and Mitochondrial Damage

Suparna Nanua and Fayth K. Yoshimura*

Department of Immunology and Microbiology and the Karmanos Cancer Institute, Wayne State University, Detroit, Michigan 48201

Received 21 October 2003/Accepted 12 January 2004

Upon inoculation into AKR mice, mink cell focus-forming murine leukemia virus (MCF MLV) accelerates thymic lymphoma formation. During the preleukemic phase of disease, we observed the induction of apoptosis in thymic lymphocytes. A similar induction of apoptosis was observed for cultured mink epithelial cells after MCF13 MLV infection. In this study, the relevance of viral pathogenicity to cell killing was determined by testing the susceptibility of various cell types from different species to lymphomagenic MLVs. We observed that the cytopathic effect of lymphomagenic MLVs was restricted to mink cells. Southern blot analysis of MLV-infected cells revealed an accumulation of the linear form of unintegrated viral DNA, particularly in mink cells after MCF13 MLV infection. Thus, a strong correlation was observed between viral superinfection, which results in the accumulation of high levels of unintegrated viral DNA, and cell killing. Immunoblot analysis for MCF13 MLV-infected mink epithelial cells did not show a significant change in total p53 levels or its phosphorylated form at Ser-15 compared with that in mock-treated cells. Moreover, a time course analysis for mink epithelial cells infected with MCF13 MLV did not reveal mitochondrial depolarization or a significant change in Bax levels. These results demonstrate that MCF13 MLV induces apoptosis preferentially in cells in which superinfection occurs, and the mechanism involved is independent of p53 activation and mitochondrial damage.

Class I mink cell focus-forming murine leukemia viruses (MCF MLVs) are the etiologic agent for the development of thymic lymphoma in AKR mice (41). The well-studied mechanism for lymphoma development is insertional mutagenesis, whereby provirus integrates proximal to a cellular oncogene, resulting in its aberrant expression (9, 11). The steps involved in the preleukemic phase of lymphoma development, however, are less well understood. We recently detected the induction of apoptosis in thymic lymphocytes of MCF13 MLV-inoculated AKR mice during the preleukemic period (49). To better understand the mechanism involved in the induction of apoptosis, we have employed cultured mink epithelial cells, which undergo a similar induction of apoptosis following virus infection (48). In these cells and thymic lymphocytes in preleukemic mice, we observed a correlation between virus-induced apoptosis and the accumulation of the linear form of unintegrated viral DNA. This accumulation of unintegrated viral DNA in infected cells is due to a phenomenon referred to as superinfection (22, 42). The ability to superinfect cells has been observed for other cytopathic retroviruses, such as subgroup B and subgroup D avian leukosis virus (ALV), reticuloendotheliosis virus (REV), and feline leukemia virus (FeLV-FAIDS) (22, 32, 42, 43). Whether the high levels of the linear form of unintegrated viral DNA that accumulate in cells as a result of superinfection play a role in cell killing is not clear. However, a potential role for unintegrated viral DNA in the induction of apoptosis is supported by recent studies which indicate that following retroviral infection, unintegrated viral DNA or integration intermediates that contain a four- to six-base gap at each end may initiate an apoptotic cascade (13, 27). Furthermore, it was demonstrated that the nonhomologous end-joining pathway, which normally repairs double-strand breaks in DNA, plays a role in the induction of apoptosis by retroviral infection (27). The hypothesis that high levels of the linear form of unintegrated viral DNA could provide an apoptotic signal is addressed in this study.

Apoptosis classically occurs via two major pathways, (i) an extrinsic receptor-mediated pathway and (ii) an intrinsic mitochondrion-mediated stress pathway. The extrinsic pathway involves activation of caspase 8, which occurs as a result of interactions between ligand and receptor, such as Fas (CD95) and FasL (2). The intrinsic pathway on the other hand involves damage to the mitochondrial membrane, which occurs in response to stress signals, such as DNA damage (19). Cytochrome *c*, which is released from the damaged mitochondria along with procaspase 9, and Apaf-1 constitute a holoenzyme complex referred to as an apoptosome that facilitates caspase 9 activation (28). The Bcl-2 family of proteins, such as Bax and Bcl-2, regulates the extent of damage to the mitochondrial membrane (12). Following genotoxic stress, Bax is activated, resulting in depolarization of the mitochondrial membrane and release of cytochrome *c* (10).

p53, a major protein involved in the intrinsic pathway, is commonly activated in response to genotoxic stress or DNA damage (21, 26). Mdm2, a negative regulator of p53, binds tightly at the amino terminus of p53, thereby promoting its rapid proteosomal degradation (25). Disruption of the Mdm2/p53 complex is produced by phosphorylation at the amino terminus of p53, which leads to stabilization of p53 and an increase in its total level (40). Phosphorylation of serine 15 (Ser-15) at the amino terminus has been shown to alleviate the inhibitory effects of Mdm2 (38). Moreover, phosphorylation of Ser-15 has been demonstrated to be an early cellular response

* Corresponding author. Mailing address: Department of Immunology and Microbiology, Wayne State University, 540 E. Canfield Ave., Detroit, MI 48201. Phone: (313) 577-1571. Fax: (313) 577-1155. E-mail: fyoshi@med.wayne.edu.

following genotoxic stress or DNA damage (40). Once activated, p53, which is a DNA-binding protein, regulates the transcription of target genes, including p21, Mdm2, Gadd45, and Bax, which are either involved in cell cycle arrest or apoptosis (14).

For many retroviruses that induce immunodeficiencies, such as FeLV-FAIDS and human immunodeficiency virus (HIV), cell killing has been demonstrated to be a critical step in viral pathogenesis (31, 36). Although not well understood, a similar correlation between cell killing and viral pathogenesis has been reported for oncogenic retroviruses, such as ALV, REV, and Moloney and SL3-3 MLV (4, 22, 37, 44). In the present study, we demonstrate for lymphomagenic MCF MLVs that, similar to other oncogenic retroviruses, cell killing strongly correlates with viral pathogenicity and superinfection. The viral cell killing we observed was species specific but appeared to be independent of cell type for the cell lines we tested. We also demonstrate that the mechanism involved in virus-induced cell killing occurs independently of p53 activation and mitochondrial membrane damage. These results indicate that the high levels of unintegrated viral DNA in virus-infected cells do not activate the intrinsic apoptotic pathway.

MATERIALS AND METHODS

Cell lines and viruses. Mink fibroblast (ATCC CCL64.1) and mink epithelial (ATCC CCL64) cells were maintained in Dulbecco's modified Eagle's medium (DMEM) supplemented with 10% heat-inactivated fetal bovine serum (Omega Scientific, Tarzana, Calif.), 1% penicillin-streptomycin, 2 mM L-glutamine, and 1 mM sodium pyruvate. Human kidney epithelial cell (293T), NIH mouse fibroblast (NIH 3T3), *Mus dunni* tail fibroblast (MDTF), and rat kidney epithelial (NRK) cells were grown in DMEM supplemented with 10% heat-inactivated fetal bovine serum and 1% penicillin-streptomycin. MLV stocks were prepared from supernatant collected from chronically infected cells. Viral titers were determined by an indirect immunofluorescence focus assay as previously described (48).

Virus infection and cell viability assay. Cells were plated in 24-well plates 1 day before virus infection. Subsequently, cells were infected with different MLVs at an appropriate multiplicity of infection (MOI) in the presence of 2 μg of Polybrene per ml. Mock-treated cells were incubated with DMEM and Polybrene. After incubation for 6 h at 37°C, viral supernatants were removed, cells were washed once with phosphate-buffered saline, and fresh medium was added. Starting at day 2 postinfection, viable cell number was enumerated by trypan blue dye exclusion and a hemacytometer.

Hirt extraction of unintegrated viral DNA. At selected time points, Hirt extraction was performed on virus-infected cells as described previously (50). Briefly, trypsinized cells were resuspended in 400 μl of 0.5 M Tris-EDTA buffer (5 mM Tris-HCl [pH 8.0], 0.5 mM EDTA). Cells were lysed in 1% sodium dodecyl sulfate solution and incubated for 30 min at 37°C. Cell lysates were gently mixed with NaCl to a final concentration of 0.9 M and incubated overnight at 4°C. Subsequently, lysates were centrifuged at 16,000 × *g* at 4°C for 30 min. Supernatant consisting of low-molecular-weight DNA was removed, and the pellet containing high-molecular-weight genomic DNA was resuspended in 0.5 M Tris-EDTA buffer. Both supernatant and pellet were treated with 50 μg each of RNase A and proteinase K prior to extraction with phenol-chloroform. DNA solutions were made to a final concentration of 0.3 M sodium acetate and 60 μg of glycogen, to which 2 volumes of ice-cold ethanol was added. Precipitated genomic DNA was dissolved in 25 μl of Tris-EDTA buffer (10 mM Tris-HCl [pH 8.0], 10 mM EDTA) and quantified by measuring the optical density at 260 nm with a spectrophotometer (Spectronics Instruments, Rochester, N.Y.).

Southern blot analysis of Hirt-extracted DNA. Hirt-extracted DNA was electrophoresed through 0.8% agarose gels in TBE buffer (89 mM Tris-borate [pH 8.0], 2 mM EDTA) at 100 V for 4 to 5 h at room temperature (RT). DNA was transferred to positively charged nylon membrane (Nytran N; Schleicher & Schuell, Keene, N.H.) by using a vacuum blotter according to the manufacturer's instructions (Bio-Rad Laboratories, Hercules, Calif.) and immobilized by UV cross-linking (Spectronics Corporation, Westbury, N.Y.). An 8.2-kb linear plasmid corresponding to the complete MCF13 MLV genome was ^{32}P-labeled with a random priming kit (Boehringer Mannheim, Indianapolis, Ind.), and a total of 5×10^6 cpm was used for overnight hybridization at 68°C. Radiolabeled probe was removed, and the membrane was washed as previously described (45). Membrane was exposed to a phosphorimager screen, and analysis was done on a Storm Scanner 840 (Molecular Dynamics, Sunnyvale, Calif.). Calculation of the copy number per cell of linear unintegrated viral DNA (UVD) was made by comparing band intensities measured from Southern blots using the ImageQuant software (Molecular Probes, Eugene, Oreg.) against a standard curve plotted from the intensities of known amounts of a purified plasmid DNA fragment comprising the complete MCF13 MLV genome (46). To obtain the copy number per cell, we divided the UVD value by the total cell number.

Immunoblotting. Cells were trypsinized and incubated in lysis buffer (20 mM HEPES [pH 7.9], 0.4 M NaCl, 1 mM EDTA, 1 mM EGTA, 25% glycerol, 2 mM dithiothreitol, 0.5 mM phenylmethylsulfonyl fluoride, 5 μg of leupeptin per ml, and 1% NP-40) at 4°C for 20 min. Lysates were centrifuged at 14,000 × *g* for 10 min at 4°C, and supernatant was collected. The amount of total protein in lysates was measured by using the bicinchoninic acid protein assay (Pierce, Rockford, Ill.). For positive controls, cellular extracts were prepared from mink epithelial cells exposed to 20 mM hydroxyurea for 16 h, 20 Gy of γ-irradiation, or 100 mJ of UV irradiation. Twenty to 30 μg of total cellular protein was electrophoresed through a 10% sodium dodecyl sulfate-polyacrylamide gel electrophoresis gel. Protein was transferred to polyvinylidene fluoride transfer membrane (Bio-Rad Laboratories) at 350 mA for 2 h. Membranes were treated with 5% blocking buffer (Tris-buffered saline [TBS; 20 mM Tris-HCl, pH 7.6; 150 mM NaCl], 5% nonfat dried milk, and 0.1% Tween 20) at RT for 1 h. Membranes were incubated overnight with primary antibody in blocking buffer at 4°C. Sources of the primary antibodies used were as follows: anti-p53 (Oncogene, La Jolla, Calif.), anti-phospho-p53 (Ser-15) (Cell Signaling, Beverly, Mass.); anti-Bax (BD Bioscience, Palo Alto, Calif.); anti-actin (Sigma, St. Louis, Mo.). Membranes were washed with TBS-T (TBS containing 0.1% Tween 20) three times and incubated with horseradish peroxidase-conjugated secondary antibody at RT for 2 h. Membranes were washed with TBS-T three times and developed with the ECL detection system (Amersham Pharmacia Biotech, Piscataway, N.J.).

Mitochondrial staining. Cells grown on glass coverslips were infected with MCF13 MLV at an MOI of 5 for 6 h at 37°C. After the virus was removed, cells were washed two times and fresh medium was added. At selected time points, cells were stained with 200 nM MitoTracker Red (Molecular Probes) for 15 min at 37°C. After removal of dye, cells were washed two times with phosphate-buffered saline and fixed with cold methanol for 5 min. Analysis of cells was done with a Zeiss Axiophot fluorescence microscope.

RESULTS AND DISCUSSION

Mink epithelial cell killing correlates with viral pathogenicity. MCF13 MLV generates thymic lymphoma beginning at approximately 10 weeks after inoculation into neonatal AKR mice (47). During the preleukemic period, our investigators have detected the depletion of virus-infected thymic lymphocytes via apoptosis (49). To better study the mechanism of cell killing by MCF13 MLV, our investigators established an in vitro system in which mink epithelial cells undergo apoptosis upon virus infection (48). To examine the relevance of mink epithelial cell killing to viral pathogenicity, we compared the ability of other oncogenic as well as nononcogenic MLVs to kill these cells. Cell killing assays were performed with MCF247 MLV, another pathogenic virus that also induces thymic lymphoma with similar kinetics to MCF13 MLV (6). A decrease in the number of viable mink epithelial cells infected with MCF247 MLV was detectable beginning at 3 days postinfection compared with mock-treated cells (Fig. 1A). Cell killing was furthermore dependent on the MOI. Mink cell killing by MCF13 MLV at an MOI of 7 was included for comparison. We observed that at a comparable MOI, MCF247 MLV was slightly more cytopathic than MCF13 MLV.

Mink epithelial cells were also infected with the nonpathogenic NZB-9 xenotropic MLV or a long terminal repeat mutant of MCF13 MLV (Mut-MCF13 MLV), which has attenu-

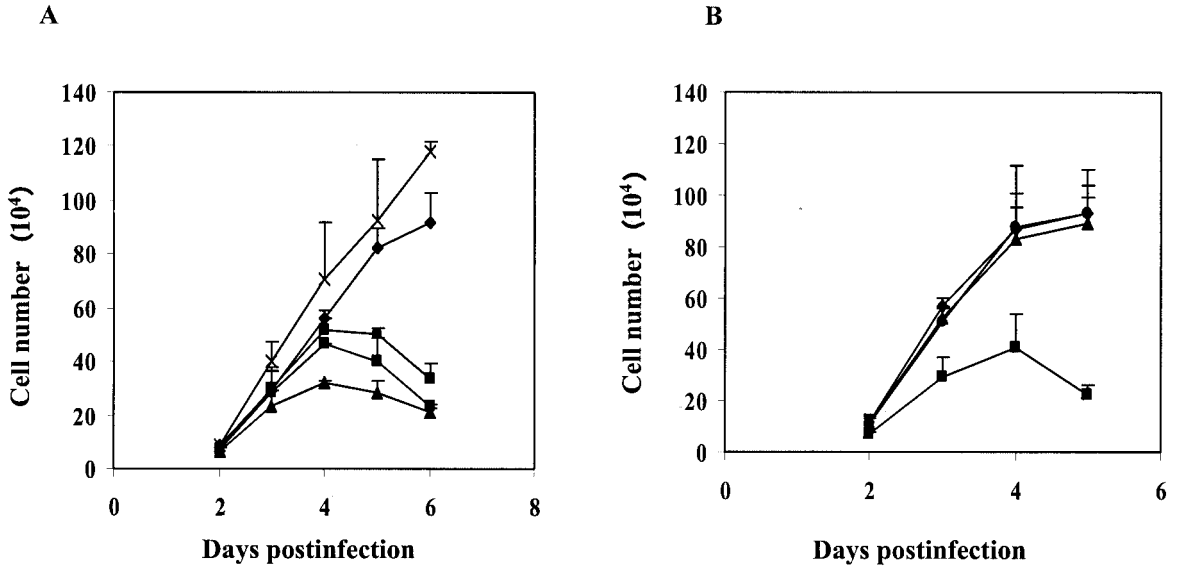

FIG. 1. Effect of MLV infection on mink epithelial cell growth. (A) Mink epithelial cells were infected with either MCF247 MLV at an MOI of 1 (●) or 7 (▲), MCF13 MLV at an MOI of 7 (■), or Mut-MCF13 MLV at an MOI of 7 (X). Growth of mock-infected cells is also shown (◆). (B) Mink epithelial cells were infected with NZB-9 MLV at an MOI of 1 (●) or 7 (▲) or MCF13 MLV at an MOI of 7 (■) or were mock infected with medium (◆). Cells were trypsinized at the indicated days after infection, and viable cells were enumerated by trypan blue dye exclusion. Values represent the means and standard deviations calculated from counting duplicate samples from two independent experiments.

ated pathogenicity (47) (Fig. 1). These viruses have similar cellular receptor usage as class I MCF MLVs, such as MCF13 and MCF247 MLV (29). Unlike our observations for these class I MCF MLVs, infection of mink epithelial cells by NZB-9 and Mut-MCF13 MLV did not produce a change in the number of viable cells over time compared with mock-infected cells. Our data demonstrate that the ability of an MLV to kill mink epithelial cells strongly correlates with viral pathogenicity. Because the cellular receptor usage for NZB-9 and Mut-MCF13 MLV is similar to that of wild-type MCF13 and MCF247 MLV, the virus-induced cell killing of mink epithelial cells does not appear to be initiated by viral glycoprotein and cellular receptor interactions at the cell surface.

Differential cell killing by lymphomagenic MCF MLVs. In our demonstration that lymphomagenic MCF MLVs are able to induce cytopathic effects, we have so far used a single cell type, i.e., mink epithelial cells. MCF MLVs are polytropic viruses that are capable of infecting cells from different species (15). Thus, to determine whether lymphomagenic MCF MLVs are cytopathic for cells of different types from various species, we performed cell killing assays on cells of mink (mink fibroblasts), mouse (*M. dunni* and NIH 3T3 fibroblasts), rat (NRK epithelial cells), and human (293T epithelial cells) origin. The results of this study are summarized in Table 1. The susceptibility of mink fibroblasts to cell killing by oncogenic and nononcogenic MLVs was similar to that observed with mink epithelial cells. Our results for mink cells thus indicate that the cell killing induced by lymphomagenic MCF MLVs is independent of cell lineage. For MCF13 and MCF247 MLV, we did not observe a significant decrease in the number of viable cells over time for any of the additional cell lines tested in comparison to mock-treated cells. Although for some cell types such as *M. dunni* and NIH 3T3 fibroblasts we used a substantially higher MOI of 100 for MCF13 and MCF247 MLV infection, we still did not observe a significant decrease in viable cell counts compared to mock-treated cells (data not shown). These results suggest a preferential cell killing of the mink cells that we tested by lymphomagenic MCF MLVs. However, because we have observed that thymic lymphocytes in AKR mice inoculated with MCF13 MLV undergo apoptosis, this virus is clearly able to kill some murine cells. Therefore, our data suggest that the cytopathic effect of this virus on murine cells is strain dependent.

Correlation between the amount of linear unintegrated viral DNA and cell killing by lymphomagenic MCF MLVs. A correlation between the accumulation of the linear form of UVD and cytopathicity has been previously reported for other pathogenic retroviruses (22, 43). The phenomenon of superinfection of a cell is indicated by the accumulation of unintegrated viral DNA. Our investigators have also detected high levels of UVD in mink epithelial cells infected with MCF13 MLV, which indicated viral superinfection (48). To determine whether superinfection correlates with cell killing by lymphomagenic

TABLE 1. Effect of MLV infection on growth of cells of different types and species

MLV	% Live cells[a]					
	Mink epithelial	Mink fibroblast	*M. dunni* fibroblast	NIH 3T3 fibroblast	293T epithelial	NRK epithelial
MCF13	38.7	26.15	88.0	98.5	91.2	94.7
MCF247	28.5	32.3	84.0	100.0	ND	93.35
Mut-MCF13	100.0	82.0	100.0	ND	ND	ND

[a] Cells were infected with MCF13 MLV, MCF247 MLV, or Mut-MCF13 MLV or mock treated. Viable cells were enumerated by trypan blue exclusion at day 5 postinfection by counting duplicate samples from two independent experiments. The percentage of viable cells was calculated from the number of mock-treated cells. ND, not determined.

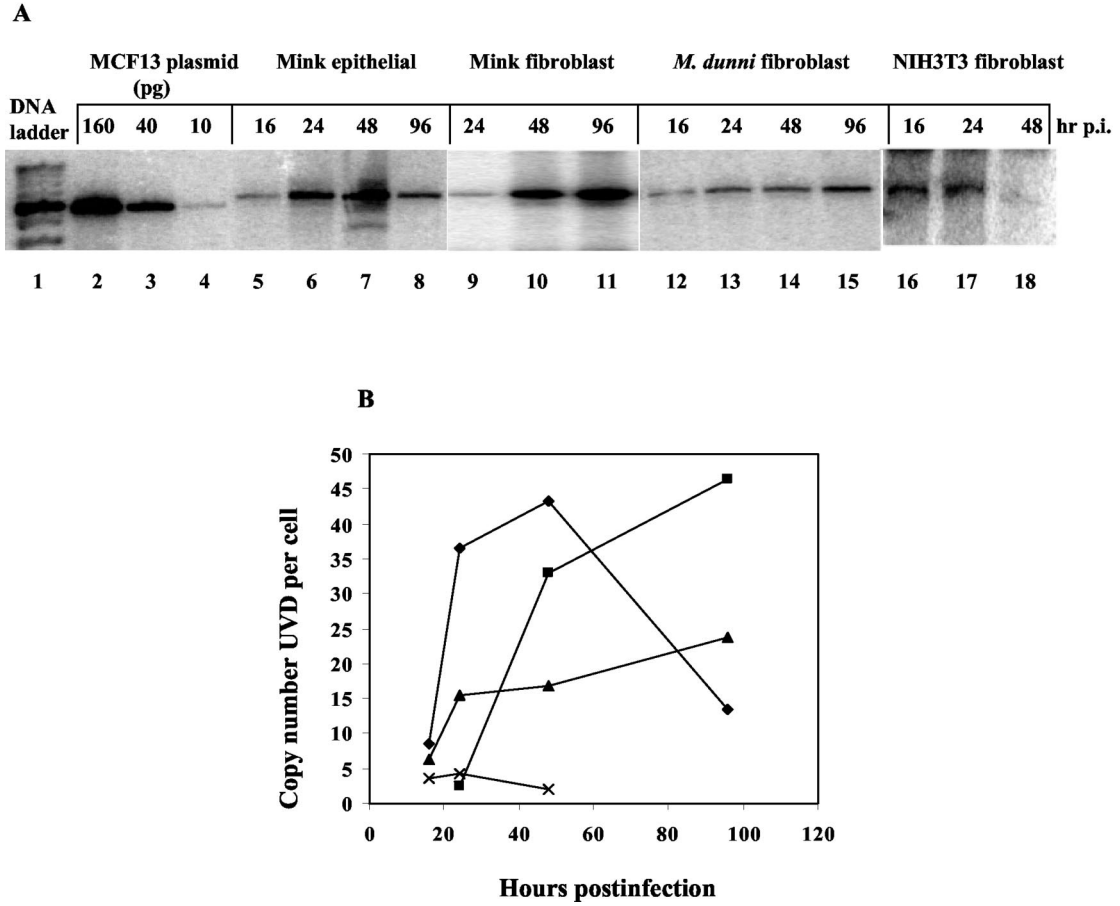

FIG. 2. High levels of linear UVD in mink cells compared with levels in *M. dunni* and NIH 3T3 fibroblasts after MCF13 MLV infection. (A) Southern blot analysis of Hirt-extracted DNA from MCF13 MLV-infected mink epithelial cells (lanes 5 to 8), mink fibroblasts (lanes 9 to 11), and *M. dunni* fibroblasts (lanes 12 to 15) at an MOI of 0.5 and from NIH 3T3 fibroblasts (lanes 16 to 18) at an MOI of 7 at the indicated hours postinfection (hr p.i.). Plasmid DNA corresponding to 160, 40, and 10 pg of genomic-length MCF13 MLV was electrophoresed in lanes 2, 3, and 4, respectively. Hybridization was done with a ^{32}P-labeled 8.2-kb length of MCF13 MLV genomic DNA. Lane 1 contains the DNA ladder. (B) Copy number per cell of the linear form of UVD over time for MCF13 MLV-infected mink epithelial cells (◆), mink fibroblasts (■), *M. dunni* fibroblasts (▲), and NIH 3T3 fibroblasts (X). Data are representative of at least two independent experiments.

MCF MLVs, we assessed the copy number of UVD per cell, as described in Materials and Methods, after infection of different cell types with MLVs with differing pathogenicities.

For mink epithelial cells infected with MCF13 MLV, the copy number of UVD per cell increased from approximately 8 copies per cell at 16 h postinfection to 43 copies per cell at 48 h postinfection, at which time the peak of UVD was detectable (Fig. 2). Similarly, the copy number of UVD per mink fibroblast increased from 2.5 copies per cell at 24 h postinfection to approximately 46 copies per cell at 96 h postinfection, resulting in an approximately 18-fold increase over this time period (Fig. 2). Although UVD was also detectable in *M. dunni* fibroblasts infected with MCF13 MLV at an MOI comparable to that of mink epithelial and fibroblast cells, the highest copy number per cell of UVD was significantly lower than that for either mink cell type (Fig. 2B). In NIH 3T3 fibroblasts infected with MCF13 MLV, the levels of detectable UVD per cell were even lower than for *M. dunni* fibroblasts (Fig. 2). The copy number of UVD per cell in NIH 3T3 fibroblasts at 48 h postinfection was less than 1, which was 40-fold lower than that for MCF13 MLV-infected mink epithelial cells at this time point (Fig. 2B). We detected similar high levels of UVD in mink fibroblast and epithelial cells infected with MCF247 MLV (data not shown).

To compare a nonpathogenic MLV, we performed a time course analysis of mink epithelial cells infected with NZB-9 MLV (Fig. 3A). At 48 h postinfection with NZB-9 MLV, the UVD copy number per cell was approximately 17-fold lower than that for MCF13 MLV (Fig. 3B). A higher MOI of 1.2 was used for NZB-9 MLV, compared with 0.5 for MCF13 MLV infection, because we did not detect any signal for NZB-9 MLV UVD on Southern blotting at lower MOIs. Thus, at the MOI used for MCF13 MLV, it is highly likely that the UVD for NZB-9 MLV would be even lower. The absence of cytopathic effects by the nonpathogenic NZB-9 MLV in mink epithelial cells correlates with its inability to superinfect these cells, as indicated by UVD levels. These results thus demonstrate that virus superinfection, as indicated by the accumulation of high levels of unintegrated viral DNA, correlates with cell killing. A similar correlation between superinfection and cell killing has been reported for other pathogenic retroviruses, such as ALV subgroups B and D, REV, and FeLV-FAIDS (22, 32, 43).

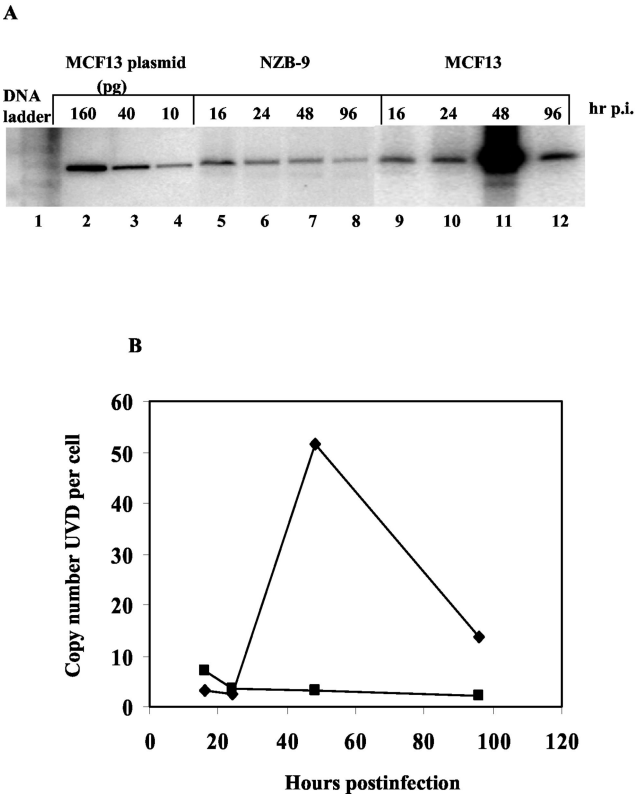

FIG. 3. Low levels of linear UVD in mink epithelial cells infected with NZB-9 MLV. (A) Southern blot analysis of Hirt-extracted DNA from mink epithelial cells infected with NZB-9 MLV at an MOI of 1.2 (lanes 5 to 8) or MCF13 MLV at an MOI of 0.5 (lanes 9 to 12) was performed at the indicated hours postinfection (hr p.i.). Lanes 2, 3, and 4 consist of 160, 40, and 10 pg, respectively, of plasmid DNA corresponding to genomic-length MCF13 MLV. Lane 1 contains a DNA ladder. (B) Copy number per mink epithelial cell of the linear form of UVD for either MCF13 MLV at an MOI of 0.5 (◆) or NZB-9 MLV at an MOI of 1.2 (■) at the indicated times after virus infection. Data are representative of two independent experiments.

MCF13 MLV infection does not result in p53 activation. It is possible that the high levels of UVD that accumulate in mink cells due to viral superinfection may be perceived as DNA with a double-strand break and thus initiate apoptosis. This hypothesis was supported by a study which showed that high levels of linear unintegrated viral DNA produced by Moloney MLV and HIV were sufficient to promote apoptosis in cells that were deficient in the DNA repair pathway involving nonhomologous end joining (27).

DNA damage or genotoxic stress most frequently induces apoptosis via a p53-dependent mechanism (7). Known to be a guardian of genomic integrity, p53 is activated upon DNA damage, which can result in either growth arrest or apoptosis (8). Following genotoxic stress, the levels of total p53 increase mainly due to stabilization of the protein and thereby an increase in its half-life (40). p53 stabilization occurs as a result of posttranslational modifications, such as phosphorylation at specific serine/threonine residues (1). It has been observed that phosphorylation of Ser-15 at the amino terminus of p53 specifically occurs following DNA damage by such agents as γ-irradiation, UV light, and hydroxyurea. The involvement of p53 in the induction of cell killing has been recently demonstrated for other retroviruses, such as HIV-1 and ts-1 Moloney MLV (5, 18, 23). Therefore, we tested the hypothesis that high levels of MCF13 MLV UVD can activate the intrinsic DNA damage pathway through p53 activation. We measured both total and phosphorylated p53 in mink epithelial cells either infected with MCF13 MLV or mock treated (Fig. 4A). We did not observe a significant difference in the total levels of p53 between virus-infected and mock-treated mink cells over time (Fig. 4A, lanes 1 to 12). To verify that mink epithelial cells are capable of responding to a known DNA damaging agent, we analyzed total cellular extracts obtained from γ-irradiated cells. We detected an approximately fivefold increase in the amount of total p53 in γ-irradiated cells compared with untreated cells (Fig. 4A, lanes 13 and 14). Thus, these results indicate that although mink cells are able to respond to a known DNA damaging agent by an increase in p53 levels, a similar response was not observed after MCF13 MLV infection.

Posttranslational modifications of p53, such as phosphorylation specifically at Ser-15, are an early cellular response to different types of genotoxic stress, including DNA damage (40). Phosphorylation at Ser-15 has been shown to disrupt the Mdm2/p53 complex, resulting in stabilization of the p53 protein (38). To measure phosphorylation of p53 at Ser-15, we used a phospho-p53-specific antibody that does not cross-react with the unphosphorylated protein. No phospho-p53 was detectable for virus-infected mink cells relative to mock-treated cells over time, which further suggested the absence of activation of p53 (Fig. 4B, lanes 2 to 7 and 9 to 14). A similar analysis of total cellular extracts obtained from γ-irradiated or hydroxyurea-treated mink epithelial cells showed that p53 phosphorylated at Ser-15 was detectable with this antibody (Fig. 4B, lanes 1, 8, 16, and 18). Our ability to detect elevated levels of total p53 and phosphorylated p53 in cells undergoing DNA damage indicates that mink epithelial cells can respond in a similar manner to DNA damage as other more-well-studied cell types. We verified that p53 is not phosphorylated in response to MCF13 MLV infection by immunostaining virus-infected mink cells with a phospho-p53-specific antibody. We did not observe any difference in the staining pattern between virus-infected mink cells and mock-treated cells, although mink cells treated with hydroxyurea showed the expected nuclear staining (data not shown). Thus, these results suggest that a p53-independent mechanism is involved in the induction of apoptosis by virus infection.

MCF13 MLV infection does not produce mitochondrial damage. Genotoxic stress or DNA damage to a cell results in activation of the intrinsic pathway of apoptosis via p53-dependent or p53-independent pathways (19, 30, 34). A hallmark of this pathway of apoptosis is mitochondrial damage, which results in the release of cytochrome *c* and cell death (20). Damage to mitochondria can be assessed by measuring mitochondrial membrane permeability or depolarization by using a mitochondrion-specific dye, such as MitoTracker Red (Molecular Probes). Polarized mitochondria retain the dye and appear as punctate structures in the cell relative to depolarized mitochondria, which produce a diffuse cellular staining (3). To determine whether mitochondrial damage is an initiating apoptotic signal in MCF13 MLV-infected mink cells, we measured mitochondrial membrane permeability starting at 24 h

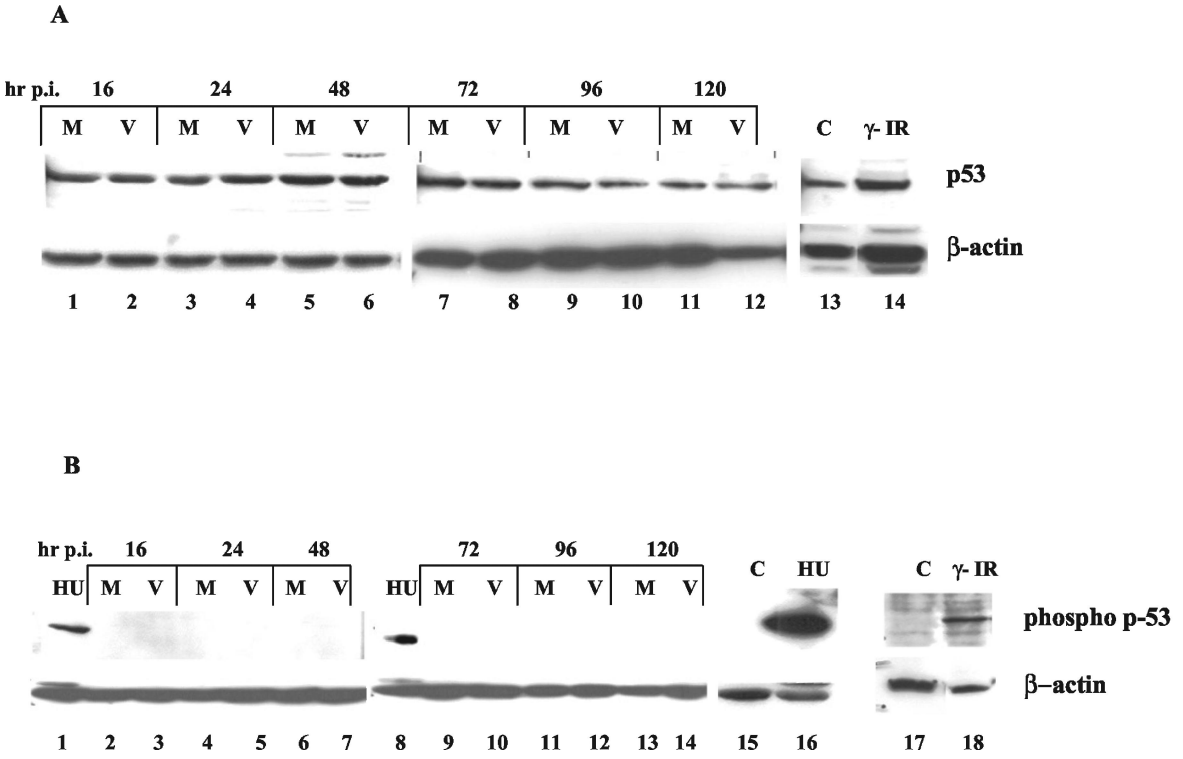

FIG. 4. MCF13 MLV infection does not result in p53 activation. (A) Western blot analysis for total p53 levels in cellular extracts from mink epithelial cells either mock treated (M; lanes 1, 3, 5, 7, 9, and 11) or infected with MCF13 MLV at an MOI of 5 (V; lanes 2, 4, 6, 8, 10, and 12) at the indicated times postinfection (hr p.i). Total cellular extracts from mink epithelial cells exposed to γ-irradiation (γ-IR; lane 14) or untreated cells (C; lane 13) were used as controls. (B) Western blot analysis for phosphorylated p53 (Ser-15) on cellular extracts from mink epithelial cells either mock treated (M; lanes 2, 4, 6, 9, 11, and 13) or infected with MCF13 MLV at an MOI of 5 (V; lanes 3, 5, 7, 10, 12, and 14) at the indicated times postinfection (hr p.i.). A phospho-p53 (Ser-15)-specific antibody was used. Total cellular extracts obtained from mink epithelial cells exposed to either 20 mM hydroxyurea (HU; lanes 1, 8, and 16) or γ-irradiation (γ-IR; lane 18) or from untreated cells (C; lanes 15 and 17) were used as controls.

postinfection. Mink cells treated with valinomycin, a potassium ionophore known to produce mitochondrial depolarization (16, 17), displayed diffuse staining compared with untreated cells (Fig. 5i and j). MitoTracker Red staining of infected mink cells over a period of 4 days produced punctate staining similar to that observed in mock-treated cells, indicating an absence of mitochondrial depolarization and damage (Fig. 5a to h). The absence of both mitochondrial damage and p53 activation indicates that the induction of apoptosis by lymphomagenic MLVs in mink epithelial cells occurs independently of the p53- and mitochondrion-mediated pathway.

The Bcl-2 family of proteins, such as Bax and Bcl-2, influence the mitochondrial membrane permeability (33). Upregulation of the proapoptotic protein Bax can result in mitochondrial depolarization (24). Therefore, to confirm the absence of mitochondrial depolarization in mink cells infected with MCF13 MLV, we also measured Bax levels of total cellular extracts by Western blotting. We did not detect a significant difference in total Bax levels in infected cells compared with mock-treated cells over time (Fig. 6, lanes 2 to 13). A similar analysis of mink epithelial cells treated with hydroxyurea showed an increase in Bax levels relative to that in untreated cells (Fig. 6, lanes 14 and 15). These results demonstrate that, unlike on exposure to known DNA damaging agents, Bax levels do not increase in mink cells after MCF13 MLV infection. Thus, these results support our conclusion that the intrinsic pathway is not involved in the induction of apoptosis in mink cells by MCF13 MLV infection.

Together, these results suggest that the high levels of unintegrated viral DNA per se do not initiate cell death but rather serve as an indicator of superinfection. Moreover, the mechanism involved in viral cell killing is independent of the intrinsic pathway of apoptosis, which involves p53 activation and mitochondrial damage. For retroviruses, such as ts-1 Moloney MLV and FeLV-FAIDS, cytopathic effects have been correlated with delayed processing and/or inefficient transport of the envelope precursor protein (35, 39). Further studies are required to determine whether a similar mechanism is involved in the induction of cell killing by lymphomagenic MLVs.

What role apoptosis of thymic lymphocytes may play in lymphomagenesis is not known. However, our recent observation that thymic lymphocytes undergo apoptosis during the preleukemic phase indicates that virus-induced tumorigenesis must involve signals that rescue these cells from apoptosis. Antiapoptotic signals could include activation of c-*myc*, which occurs in approximately 25% of thymic lymphoma cells, and upregulation of NF-κB (unpublished data). Both phenomena are involved in rescuing cells from apoptosis. One possible role of virus superinfection, which is observed in cells undergoing apoptosis, may be to increase the number of proviral integra-

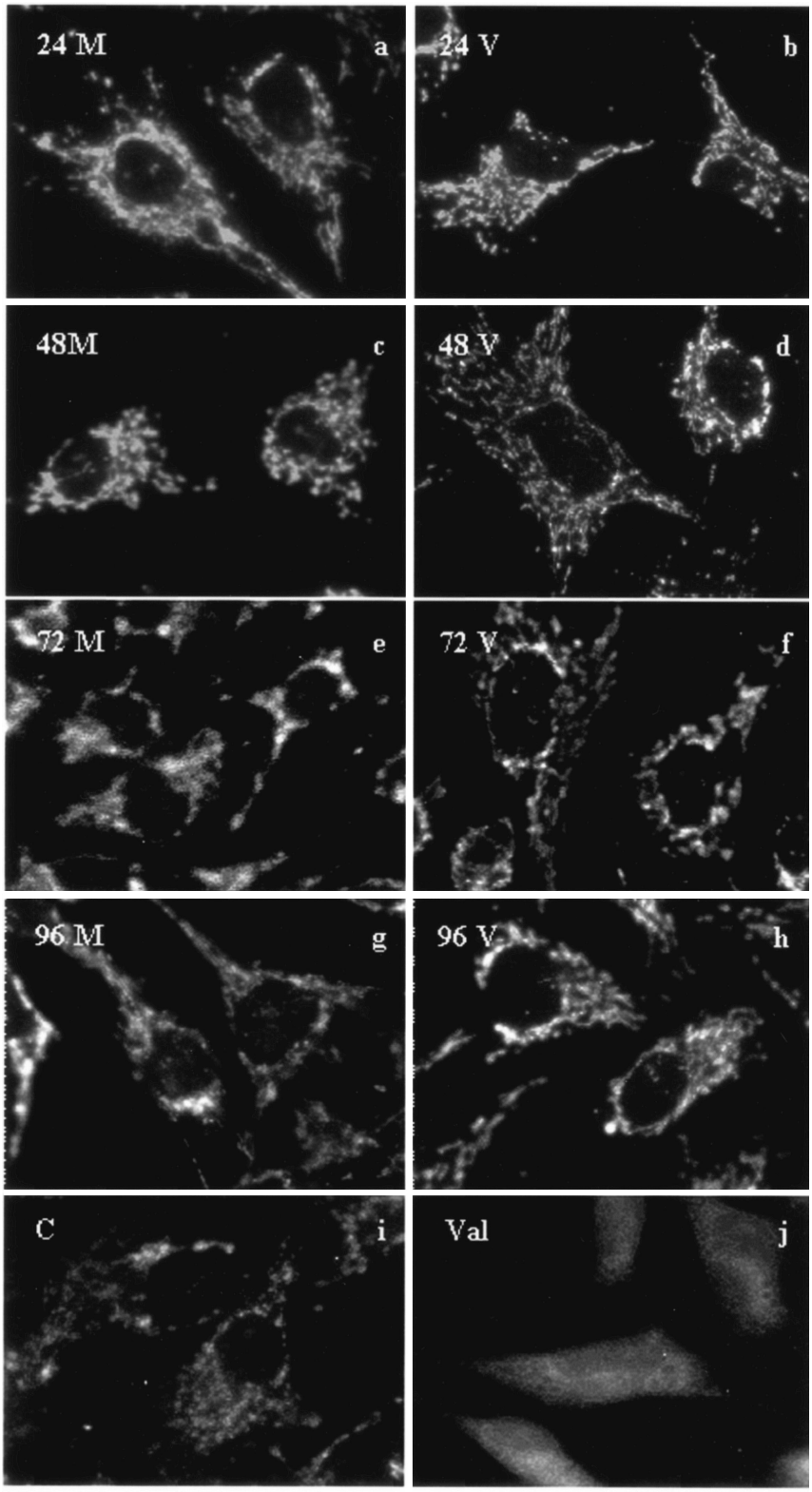

FIG. 5. Absence of mitochondrial depolarization in mink epithelial cells infected with MCF13 MLV. Mink epithelial cells were either mock treated (M; a, c, e, and g) or infected with MCF13 MLV as described for Fig. 6 (V; b, d, f, and h). At the indicated time points postinfection, cells were stained with 200 nM MitoTracker Red and imaged with a Zeiss Axiophot fluorescence microscope. Mink epithelial cells treated with 1 μg of valinomycin per ml for 1 h (Val; j) or untreated (C; i) were used as controls.

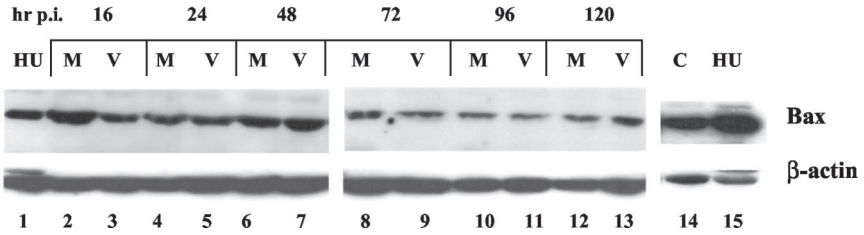

FIG. 6. No change in Bax levels was observed after MCF13 MLV infection. Results shown are from a Western blot analysis of Bax in total cellular extracts from mink epithelial cells that were either mock treated (M; lanes 2, 4, 6, 8, 10, and 12) or infected with MCF13 MLV at an MOI of 5 (V; lanes 3, 5, 7, 9, 11, and 13) at the indicated times postinfection (hr p.i.). Total cellular extracts from mink epithelial cells exposed to 20 mM hydroxyurea (HU; lanes 1 and 15) or untreated (C; lane 14) were used as controls.

tion events that lead to the upregulation of antiapoptotic genes. It is clear that further studies are required to understand the exact role of viral superinfection and apoptosis in MCF MLV tumorigenesis.

ACKNOWLEDGMENTS

We thank Xixia Luo for her excellent technical assistance. We also acknowledge T. R. Reddy for helpful comments on the manuscript. We are grateful to K. Moin and R. Haque for help in the use of the Ziess fluorescence microscope in the Karmanos Cancer Institute confocal microscopy core facility.

This work is supported by Public Health Service grant CA44166 to F.K.Y. from the National Institutes of Health.

REFERENCES

1. **Ashcroft, M., M. H. Kubbutat, and K. H. Vousden.** 1999. Regulation of p53 function and stability by phosphorylation. Mol. Cell. Biol. **19:**1751–1758.
2. **Ashkenazi, A., and V. M. Dixit.** 1998. Death receptors: signaling and modulation. Science **281:**1305–1308.
3. **Bernardi, P., L. Scorrano, R. Colonna, V. Petronilli, and F. Di Lisa.** 1999. Mitochondria and cell death. Mechanistic aspects and methodological issues. Eur. J. Biochem. **264:**687–701.
4. **Bonzon, C., and H. Fan.** 1999. Moloney murine leukemia virus-induced preleukemic thymic atrophy and enhanced thymocyte apoptosis correlate with disease pathogenicity. J. Virol. **73:**2434–2441.
5. **Castedo, M., T. Roumier, J. Blanco, K. F. Ferri, J. Barretina, L. A. Tintignac, K. Andreau, J. L. Perfettini, A. Amendola, R. Nardacci, P. Leduc, D. E. Ingber, S. Druillennec, B. Roques, S. A. Leibovitch, M. Vilella-Bach, J. Chen, J. A. Este, N. Modjtahedi, M. Piacentini, and G. Kroemer.** 2002. Sequential involvement of Cdk1, mTOR and p53 in apoptosis induced by the HIV-1 envelope. EMBO J. **21:**4070–4080.
6. **Chattopadhyay, S. K., M. R. Lander, S. Gupta, E. Rands, and D. R. Lowy.** 1981. Origin of mink cytopathic focus-forming (MCF) viruses: comparison with ecotropic and xenotropic murine leukemia virus genomes. Virology **113:**465–483.
7. **Chernov, M. V., and G. R. Stark.** 1997. The p53 activation and apoptosis induced by DNA damage are reversibly inhibited by salicylate. Oncogene **14:**2503–2510.
8. **Choisy-Rossi, C., P. Reisdorf, and E. Yonish-Rouach.** 1998. Mechanisms of p53-induced apoptosis: in search of genes which are regulated during p53-mediated cell death. Toxicol. Lett. **102–103:**491–496.
9. **Corcoran, L. M., J. M. Adams, A. R. Dunn, and S. Cory.** 1984. Murine T lymphomas in which the cellular myc oncogene has been activated by retroviral insertion. Cell **37:**113–122.
10. **Cory, S., and J. M. Adams.** 2002. The *Bcl*II family: regulators of the cellular life-or-death switch. Nat. Rev. Cancer **2:**647–656.
11. **Cory, S., S. Gerondakis, L. M. Corcoran, O. Bernard, E. Webb, and J. M. Adams.** 1984. Activation of the c-myc oncogene in B and T lymphoid tumors. Curr. Top. Microbiol. Immunol. **113:**161–165.
12. **Craig, R. W.** 1995. The bcl-2 gene family. Semin. Cancer Biol. **6:**35–43.
13. **Daniel, R., R. A. Katz, and A. M. Skalka.** 1999. A role for DNA-PK in retroviral DNA integration. Science **284:**644–647.
14. **el-Deiry, W. S., S. E. Kern, J. A. Pietenpol, K. W. Kinzler, and B. Vogelstein.** 1992. Definition of a consensus binding site for p53. Nat. Genet. **1:**45–49.
15. **Evans, L. H., R. P. Morrison, F. G. Malik, J. Portis, and W. J. Britt.** 1990. A neutralizable epitope common to the envelope glycoproteins of ecotropic, polytropic, xenotropic, and amphotropic murine leukemia viruses. J. Virol. **64:**6176–6183.
16. **Felber, S. M., and M. D. Brand.** 1982. Valinomycin can depolarize mitochondria in intact lymphocytes without increasing plasma membrane potassium fluxes. FEBS Lett. **150:**122–124.
17. **Furlong, I. J., C. Lopez Mediavilla, R. Ascaso, A. Lopez Rivas, and M. K. Collins.** 1998. Induction of apoptosis by valinomycin: mitochondrial permeability transition causes intracellular acidification. Cell Death Differ. **5:**214–221.
18. **Genini, D., D. Sheeter, S. Rought, J. J. Zaunders, S. A. Susin, G. Kroemer, D. D. Richman, D. A. Carson, J. Corbeil, and L. M. Leoni.** 2001. HIV induces lymphocyte apoptosis by a p53-initiated, mitochondrial-mediated mechanism. FASEB J. **15:**5–6.
19. **Green, D. R.** 1998. Apoptotic pathways: the roads to ruin. Cell **94:**695–698.
20. **Green, D. R., and J. C. Reed.** 1998. Mitochondria and apoptosis. Science **281:**1309–1312.
21. **Kastan, M. B., O. Onyekwere, D. Sidransky, B. Vogelstein, and R. W. Craig.** 1991. Participation of p53 protein in the cellular response to DNA damage. Cancer Res. **51:**6304–6311.
22. **Keshet, E., and H. M. Temin.** 1979. Cell killing by spleen necrosis virus is correlated with a transient accumulation of spleen necrosis virus DNA. J. Virol. **31:**376–388.
23. **Kim, H. T., S. Tasca, W. Qiang, P. K. Wong, and G. Stoica.** 2002. Induction of p53 accumulation by Moloney murine leukemia virus-ts1 infection in astrocytes via activation of extracellular signal-regulated kinases 1/2. Lab. Investig. **82:**693–702.
24. **Kitada, S., S. Krajewski, T. Miyashita, M. Krajewska, and J. C. Reed.** 1996. Gamma-radiation induces upregulation of Bax protein and apoptosis in radiosensitive cells in vivo. Oncogene **12:**187–192.
25. **Lakin, N. D., and S. P. Jackson.** 1999. Regulation of p53 in response to DNA damage. Oncogene **18:**7644–7655.
26. **Lane, D. P.** 1992. Cancer. p53, guardian of the genome. Nature **358:**15–16.
27. **Li, L., J. M. Olvera, K. E. Yoder, R. S. Mitchell, S. L. Butler, M. Lieber, S. L. Martin, and F. D. Bushman.** 2001. Role of the non-homologous DNA end joining pathway in the early steps of retroviral infection. EMBO J. **20:**3272–3281.
28. **Li, P., D. Nijhawan, I. Budihardjo, S. M. Srinivasula, M. Ahmad, E. S. Alnemri, and X. Wang.** 1997. Cytochrome c and dATP-dependent formation of Apaf-1/caspase-9 complex initiates an apoptotic protease cascade. Cell **91:**479–489.
29. **Marin, M., C. S. Tailor, A. Nouri, S. L. Kozak, and D. Kabat.** 1999. Polymorphisms of the cell surface receptor control mouse susceptibilities to xenotropic and polytropic leukemia viruses. J. Virol. **73:**9362–9368.
30. **Merritt, A. J., T. D. Allen, C. S. Potten, and J. A. Hickman.** 1997. Apoptosis in small intestinal epithelial from p53-null mice: evidence for a delayed, p53-independent G_2/M-associated cell death after gamma-irradiation. Oncogene **14:**2759–2766.
31. **Meyaard, L., S. A. Otto, R. R. Jonker, M. J. Mijnster, R. P. Keet, and F. Miedema.** 1992. Programmed death of T cells in HIV-1 infection. Science **257:**217–219.
32. **Mullins, J. I., C. S. Chen, and E. A. Hoover.** 1986. Disease-specific and tissue-specific production of unintegrated feline leukaemia virus variant DNA in feline AIDS. Nature **319:**333–336.
33. **Oltvai, Z. N., C. L. Milliman, and S. J. Korsmeyer.** 1993. Bcl-2 heterodimerizes in vivo with a conserved homolog, Bax, that accelerates programmed cell death. Cell **74:**609–619.
34. **Peled, A., D. Zipori, and V. Rotter.** 1996. Cooperation between p53-dependent and p53-independent apoptotic pathways in myeloid cells. Cancer Res. **56:**2148–2156.
35. **Poss, M. L., S. W. Dow, and E. A. Hoover.** 1992. Cell-specific envelope glycosylation distinguishes FIV glycoproteins produced in cytopathically and noncytopathically infected cells. Virology **188:**25–32.
36. **Rojko, J. L., J. R. Hartke, C. M. Cheney, A. J. Phipps, and J. C. Neil.** 1996. Cytopathic feline leukemia viruses cause apoptosis in hemolymphatic cells. Prog. Mol. Subcell. Biol. **16:**13–43.
37. **Rulli, K., J. Lenz, and L. S. Levy.** 2002. Disruption of hematopoiesis and

thymopoiesis in the early premalignant stages of infection with SL3-3 murine leukemia virus. J. Virol. **76:**2363–2374.
38. **Shieh, S. Y., M. Ikeda, Y. Taya, and C. Prives.** 1997. DNA damage-induced phosphorylation of p53 alleviates inhibition by MDM2. Cell **91:**325–334.
39. **Shikova, E., Y. C. Lin, K. Saha, B. R. Brooks, and P. K. Wong.** 1993. Correlation of specific virus-astrocyte interactions and cytopathic effects induced by ts1, a neurovirulent mutant of Moloney murine leukemia virus. J. Virol. **67:**1137–1147.
40. **Siliciano, J. D., C. E. Canman, Y. Taya, K. Sakaguchi, E. Appella, and M. B. Kastan.** 1997. DNA damage induces phosphorylation of the amino terminus of p53. Genes Dev. **11:**3471–3481.
41. **Stoye, J. P., C. Moroni, and J. M. Coffin.** 1991. Virological events leading to spontaneous AKR thymomas. J. Virol. **65:**1273–1285.
42. **Temin, H. M., E. Keshet, and S. K. Weller.** 1980. Correlation of transient accumulation of linear unintegrated viral DNA and transient cell killing by avian leukosis and reticuloendotheliosis viruses. Cold Spring Harbor Symp. Quant. Biol. **44:**773–778.
43. **Weller, S. K., A. E. Joy, and H. M. Temin.** 1980. Correlation between cell killing and massive second-round superinfection by members of some subgroups of avian leukosis virus. J. Virol. **33:**494–506.
44. **Weller, S. K., and H. M. Temin.** 1981. Cell killing by avian leukosis viruses. J. Virol. **39:**713–721.
45. **Yoshimura, F. K., and M. Breda.** 1981. Lack of AKR ecotropic provirus amplification in AKR leukemic thymuses. J. Virol. **39:**808–815.
46. **Yoshimura, F. K., B. Davison, and K. Chaffin.** 1985. Murine leukemia virus long terminal repeat sequences can enhance gene activity in a cell-type-specific manner. Mol. Cell. Biol. **5:**2832–2835.
47. **Yoshimura, F. K., T. Wang, and M. Cankovic.** 1999. Sequences between the enhancer and promoter in the long terminal repeat affect murine leukemia virus pathogenicity and replication in the thymus. J. Virol. **73:**4890–4898.
48. **Yoshimura, F. K., T. Wang, and S. Nanua.** 2001. Mink cell focus-forming murine leukemia virus killing of mink cells involves apoptosis and superinfection. J. Virol. **75:**6007–6015.
49. **Yoshimura, F. K., T. Wang, F. Yu, H. R. Kim, and J. R. Turner.** 2000. Mink cell focus-forming murine leukemia virus infection induces apoptosis of thymic lymphocytes. J. Virol. **74:**8119–8126.
50. **Yoshimura, F. K., and R. A. Weinberg.** 1979. Restriction endonuclease cleavage of linear and closed circular murine leukemia viral DNAs: discovery of a smaller circular form. Cell **16:**323–332.